



# Lanthanide/zinc centered photoactive hybrids with functional sulfonamide linkage: Coordination bonding assembly, characterization and photophysical properties

Kai Qian, Bing Yan\*

Department of Chemistry, Tongji University, Shanghai 200092, China

## ARTICLE INFO

### Article history:

Available online 24 July 2009

### Keywords:

Organic/inorganic hybrid material  
Coordination bonding assembly  
Sulfonamide linkage  
Photophysical property

## ABSTRACT

In this paper, two novel kinds of organic–inorganic monomer, SUA-APEMS and SUA-APS, have been achieved by modifying 5-sulfosalicylic acid (SUA) with 3-aminopropyl-methyl-diethoxysilane (APEMS) and 3-aminopropyl trimethoxysilane (APS). These two organic–inorganic monomers were used as multi-functional bridged components, which can coordinate to metal ions ( $Tb^{3+}/Eu^{3+}/Zn^{2+}$ ) with carbonyl groups, strongly absorb ultraviolet and effectively transfer energy to metal ions through their triplet excited state, as well as involve in the sol–gel process with inorganic host precursor tetraethoxysilane (TEOS), resulting two series of molecular hybrid materials (named as SUA-APEMS/APS-RE) with double chemical bond (RE(Zn)–O coordination bond and Si–O covalent bond). The effective intra-molecular energy transfer process gives rise to the characteristic emission of metal ions and the chemical bond make the hybrid materials owning better properties.

© 2009 Elsevier Ltd. All rights reserved.

## 1. Introduction

Luminescent materials can be applied in many fields such as tunable laser, display and amplifier for optical communication [1]. Much research work has been focused on the lanthanide complexes for their unique luminescence properties such as broad spectral range (from ultraviolet to infrared region), particular strong narrow-width emission in the visible region and wide range of lifetimes [2,3]. The design of efficient rare-earth complexes depends on the selection of diverse classes of ligands:  $\beta$ -diketones [4–6], heterocyclic ligands [7,8], cryptands [9], calixarenes [10,11], macrocyclic ligands [12], terphenyl ligands [13], proteins [14], etc. But the poor thermal stability and mechanical property of lanthanide complexes limit their usage. Recently, in order to overcome the above-mentioned shortcomings, entrapment of rare-earth complexes with  $\beta$ -diketones, aromatic carboxylic acids, and heterocyclic ligands in inorganic host has been studied extensively because these organic–inorganic hybrid materials combine the advantages of both organic and inorganic parts. According to the interaction among the different phases in hybrid systems, these hybrid materials can be mainly divided into two major classes: class I is physically mixed with weak interactions (hydrogen bond, Van der Waals force or weak static effect); class II belongs to chemically bonded hybrids with strong covalent bonds [15–19]. However, these hybrid materials of class I have many disadvantages: the dopant concentration of lanthanide complexes is

very low, and the photoactive molecules can be easily leached, so it is hard to obtain transparent and uniform material. Poor mechanical property of them also restricts their practical application. So the present work is focused on the class II hybrid system of lanthanide complex luminescent centers bonded with a siloxane matrix through Si–O linkages. Franville et al. have concentrated on the modification of pyridine-dicarboxylic acid or their derivatives, which results in strong  $Eu^{3+}$  ions emissions due to efficient ligand-to-metal energy transfer [20]. Zhang and coworkers are focused on modification of heterocyclic ligands (1,10-phenanthroline and di-pyridine) to construct molecular-based hybrids [21,22]. Our research team has also carried out extensive work concerning the covalently bonded hybrid materials. In previous research, three methods have been used to synthesis lanthanide based optical active covalent hybrid materials: amino-modification [23,24], carboxyl-modification [25,26], and hydroxyl-modification [27,28]. As for the preparation of such hybrid materials, the sol–gel technique has proven to be a convenient synthetic method because of its unique characteristics, namely low temperature and versatility [29,30].

From these researches, it can be concluded that the critical step to prepare these hybrids is to synthesize a novel monomer as a covalent bridge between the organic and inorganic part. So the development of novel linkages for tethering organic compounds to inorganic solid supports is an area of active investigation. In this paper, a novel sulfonamide linkage is selected to link these two parts, which is based on the modification of 5-sulfosalicylic acid with APEMS and APS for sulfosalicylic acid possesses the reactive functionalized sulfo group and excellent photoactive unit. A new

\* Corresponding author. Tel.: +86 21 65984663; fax: +86 21 65982287.  
E-mail address: [byan@tongji.edu.cn](mailto:byan@tongji.edu.cn) (B. Yan).

series of luminescent hybrid molecular-based materials is achieved via a special sol–gel process. Compared with other existing materials, these kinds of hybrid materials not only provide a new modification and assembly path, but also develop a new type of rare-earth organic/inorganic hybrids.

## 2. Experimental

### 2.1. Starting materials

All the chemicals were purchased from Aldrich and used as received. All normal organic solvents were distilled before utilization according to the literature procedures. Europium and terbium nitrates were obtained from the corresponding oxides in concentrated nitric acid.

### 2.2. Modification of 5-sulfosalicylic acid to molecular bridge

About 1.016 g (4 mmol) 5-sulfosalicylic acid was dissolved in 20 mL chloroform and then 0.476 g (4 mmol)  $\text{SOCl}_2$  was added to the solution drop by drop. The mixed solution was refluxing at 120 °C for 4 h. After isolation, the residue was recrystallized by toluene. Then a yellow solid powder was obtained, named as 5-sulfosalicylic sulfonic chloride (5-SUCl). The sulfonic chloride can directly reacted with APS, APEMS in pyridine. The sulfonamide linkage was formed as follows: 4 mmol sulfonic chloride was dissolved in pyridine by stirring and 4 mmol APS or APEMS was then added to the solution by drops. The whole mixture was refluxing at 80 °C for 4 h. After isolation, a red oil sulfonamide precursor was obtained.

### 2.3. Assembly of molecular hybrid materials

The sol–gel derived hybrid material was prepared as follows (Fig. 1): sulfonamide precursor (1 mmol) was dissolved in the mixture of 5 mL DMF and 2 mL ethanol by stirring. Then 0.3 mmol RE ( $\text{NO}_3$ )<sub>3</sub>·6H<sub>2</sub>O (RE = Eu, Tb) and 2.0 mmol tetraethoxysilane (TEOS) was added into the solution. One drop of diluted hydrochloric acid was put into it to promote hydrolysis. The mixture was stirred magnetically in a covered Teflon beaker for an hour. After that it was aged at 60 °C for the gelation in 3 days. The gels were collected and ground as powder materials for the optic studies. The hybrid material containing  $\text{Zn}^{2+}$  was also prepared in the same way, but the mole ratio of  $\text{Zn}(\text{Ac})_2 \cdot 2\text{H}_2\text{O}$ : sulfonamide precursor was 1:2. Comparing with the materials containing different metal ions those hybrid materials without metal ions were also synthesized for the photophysical studies.

### 2.4. Physical measurement

All measurements were completed under room temperature. Fourier transform infrared (FTIR) spectra were measured within the 4000–400  $\text{cm}^{-1}$  region on an (Nicolet Nexus 912 AO446) infrared spectrophotometer with the KBr pellet technique. Ultraviolet absorption spectra were recorded with an Agilent 8453 spectrophotometer.  $^1\text{H}$  NMR spectra were recorded in  $\text{CDCl}_3$  on a BRUKER AVANCE-500 spectrometer with tetramethylsilane (TMS) as inter reference. Scanning electronic microscope (SEM) images were obtained with a Philips XL-30. Luminescence (excitation and emission) spectra of these solid complexes were determined with a RF-5301 spectrophotometer. Luminescence lifetime measurements were carried out on an Edinburgh FLS920 phosphorimeter using a 450 w xenon lamp as excitation source. Solid-state  $^{29}\text{Si}$  magic-angle spinning (MAS) NMR spectrum was recorded at 79.46 MHz using a Bruker Avance 400 spectrometer. The chemical shifts were quoted in ppm from tetramethylsilane.

## 3. Result and discussion

The FTIR spectra for SUCl (a), SUA-APS (b), and Tb-SUA-APS (c) are shown in Fig. 2, respectively. From the curve of the sulfonic chloride, the  $\nu_{\text{as}}(\text{O}=\text{S}=\text{O})$  and  $\nu_{\text{s}}(\text{O}=\text{S}=\text{O})$  absorption bands located at 1387 and 1251  $\text{cm}^{-1}$ . The  $\nu(\text{C}=\text{O})$  vibration was observed at 1667  $\text{cm}^{-1}$  due to the existence of  $-\text{COOH}$ . In the curve of the sulfonamide precursor (b), the grafting reaction is evidenced by the sharp band located at 1243  $\text{cm}^{-1}$  corresponding to  $\nu(\text{S}-\text{N})$  [31]. Besides the  $\nu(-\text{CH}_2-)$  located at 2932, 2860  $\text{cm}^{-1}$  and the  $\nu(\text{Si}-\text{O}-\text{C})$  located at 1099  $\text{cm}^{-1}$  further proved the occurrence of reaction.

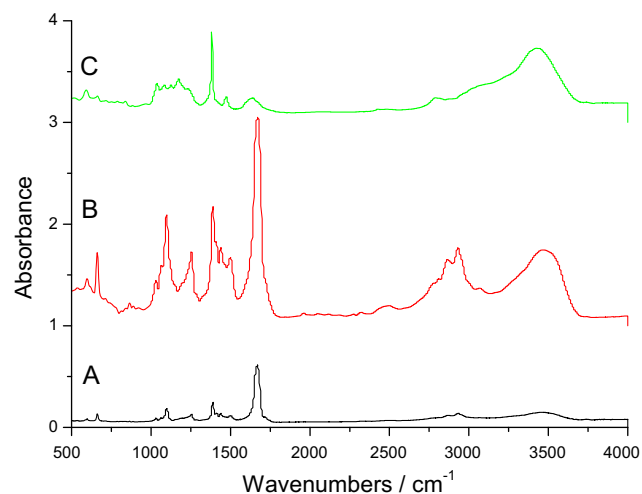


Fig. 2. The selected FTIR spectra for SUCl (A), SUA-APS (B), and Tb-SUA-APS (C).

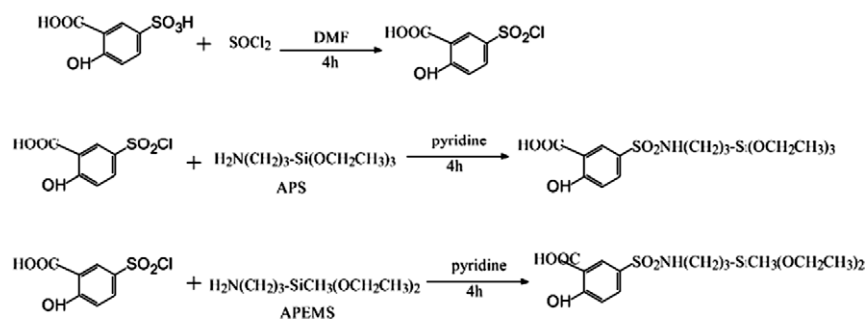


Fig. 1. Scheme of the syntheses process of SUA-APS and SUA-APEMS.

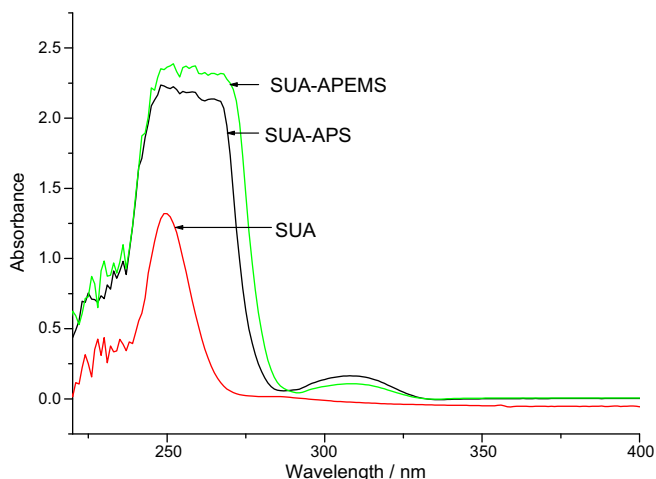


Fig. 3. The ultraviolet absorption spectra of SUA, SUA-APS, SUA-APEMS.

The  $\nu(\text{O}=\text{S}=\text{O})$  was still obviously observed at  $1377\text{ cm}^{-1}$  in the curve of the final material (c), while most other vibrations are weak. The wide absorption band at around  $1100\text{ cm}^{-1}$  indicated the dominating of  $\nu(\text{O}-\text{Si}-\text{O})$ . There exists wide band absorption at about  $3400\text{ cm}^{-1}$  in all these three curves. And the absorption band in curve c is more obvious because there were more crystal water in the final material due to the sol-gel process (the  $\nu(\text{H}-\text{O}-\text{H})$ :  $3600-3000\text{ cm}^{-1}$ ). In spectra of precursor (SUA-APS), the  $\nu(\text{C}=\text{O})$  vibration is located at  $1683\text{ cm}^{-1}$ . But in the spectra of the hybrid material (SUA-APS-Tb), the  $\nu(\text{C}=\text{O})$  vibration is shifted to the  $1629\text{ cm}^{-1}$ . The shift is a proof of the coordination of the carboxylic group to the metallic ion with the oxygen atoms [32,33].

Fig. 3 shows the ultraviolet absorption spectra of SUA, SUA-APS and SUA-APEMS. The ultraviolet absorption spectra of SUA-APS, SUA-APEMS are similar compared with the SUA. The absorption bands corresponding to the  $\pi \rightarrow \pi^*$  electronic transition are located at 249, 256, 257 nm, respectively. It is observed that a red shift of the major  $\pi \rightarrow \pi^*$  electronic transitions occurs and it is estimated that during the modification of 5-sulfosalicylic acid, the different ligand may hinder the conjugating effect of double bonds ( $\text{S}=\text{O}$ ) and decrease the energy difference levels among electron transitions. Besides the absorption peaks of the SUA-APS and SUA-APEMS are wider than that of SUA. It is also obvious that there exist absorption peaks corresponding to the  $\pi \rightarrow \pi^*$  electronic transition in the spectra of SUA-APS and SUA-APEMS, located at around 310 nm while this peak can not be seen in the spectrum of SUA. All these differences in the ultraviolet absorption spectra between SUA and the modified 5-sulfosalicylic acid indicate the success of the modification [31,33].

Besides, selected  $^{29}\text{Si}$  MAS NMR spectroscopy of Tb-SUA-APEMS is shown in Fig. 4. Distinct resonances can be observed for the siloxane [ $\text{Q}^n = \text{Si}-(\text{OSi})_n(\text{OH})_{4-n}$ ,  $n = 2-4$ ] and organosiloxane [ $\text{T}^m = \text{R}-\text{Si}-(\text{OSi})_m(\text{OH})_{3-m}$ ,  $m = 1-3$ ] species. The relative integrated intensities of the organosiloxane  $\text{T}^1$ ,  $\text{T}^2$ , and  $\text{T}^3$  NMR signals can be employed to estimate the degree of hydrolysis-condensation of organic functional groups. Compared with  $\text{T}^1$  and  $\text{T}^2$  organosiloxane centers, the predominance of  $\text{T}^3$  [the  $\text{T}^3:(\text{T}^3 + \text{T}^2 + \text{T}^1)$  ratio is 0.74] suggests that the hydrolysis and condensation of the organo functionality (BSPA-Si) in the order structure is nearly complete, indicating a strong linkage (three Si-O-Si covalent bonds) between the organic ligand and the silica matrix.

Fig. 5 shows the UV-Vis DRS of Tb-SUA-APEMS, Tb-SUA-APS. Both have broad absorption band ranging from 200 to 480 nm. The broad absorption suggests that the organic part played an

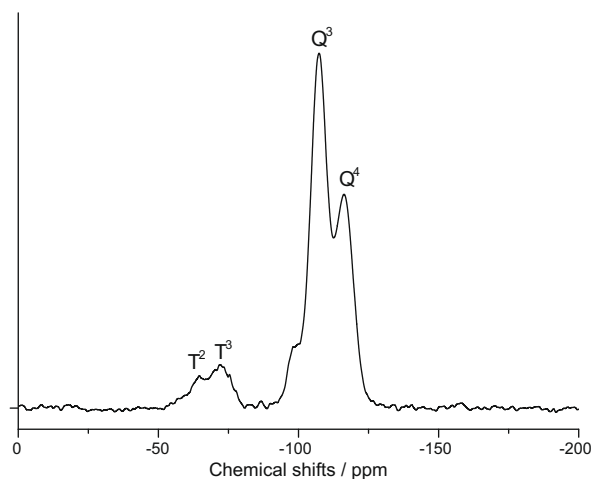


Fig. 4. The selected  $^{29}\text{Si}$  MAS NMR spectroscopy of Tb-SUA-APEMS.

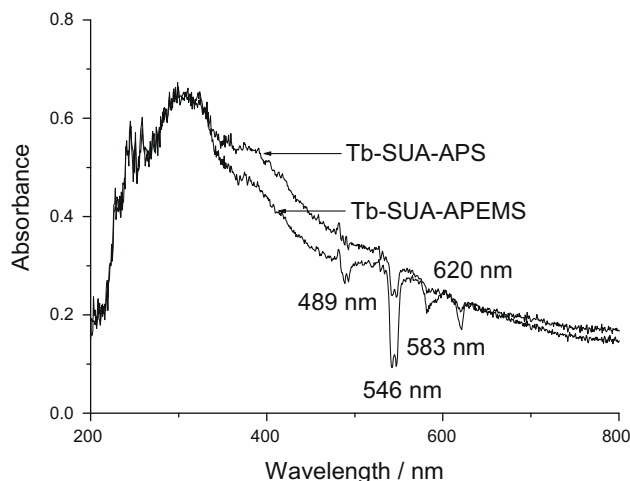


Fig. 5. The selected UV-Vis DRS of Tb-SUA-APEMS and Tb-SUA-APS.

important role in the energy absorption process. The rare-earth ions can be excited by intra-molecular energy transfer after the energy absorption process. So the broad absorption band in the short wavelength region leads to the good luminescence properties of these hybrid materials which can be proved by the emission spectrum of the materials. The negative absorption peaks corresponding to the characteristic emission peak at 489, 546, 583, 620 nm of the active terbium ions can be observed in the spectrum. These negative absorption peaks are due to the  $^5\text{D}_4-^7\text{F}_j$  transitions of the  $\text{Tb}^{3+}$  ion excited by the UV component in the incident ray during the measurement. Compared with the spectrum of SUA-APEMS-Tb, SUA-APS-Tb has the same peaks but with weaker intensities, because other emission peak of  $\text{Tb}^{3+}$  are obscure except for the characteristic peak at 546 nm [33].

Figs. 6 and 7 show the excitation and emission spectra of the chemically bonded hybrids without metal ions (SUA-APEMS, SUA-APS) and zinc hybrid materials (Zn-SUA-APEMS, Zn-SUA-APS). For Fig. 6, both excitation and emission spectra of the two hybrids without metal ions show the broad bands, 130 nm range (from 220 to 350 nm) excitation band and 200 nm range (from 350 to 550 nm) emission band, respectively. The excitation spectra of SUA-APEMS and SUA-APS are similar except for the distinction of intensity, suggesting the same typical characteristic of organic molecule units of SUA. But the emission spectra of them are different in spite of the 200 nm range. SUA-APEMS hybrid material

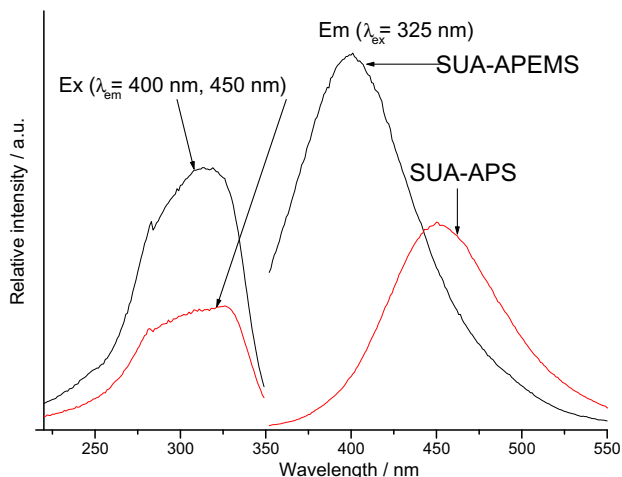


Fig. 6. The emission spectra of the non-metallic hybrid materials.

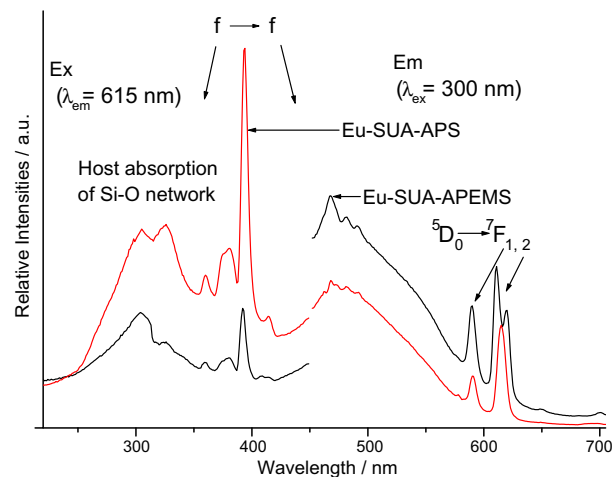


Fig. 8. The emission spectra of the europium hybrid materials.

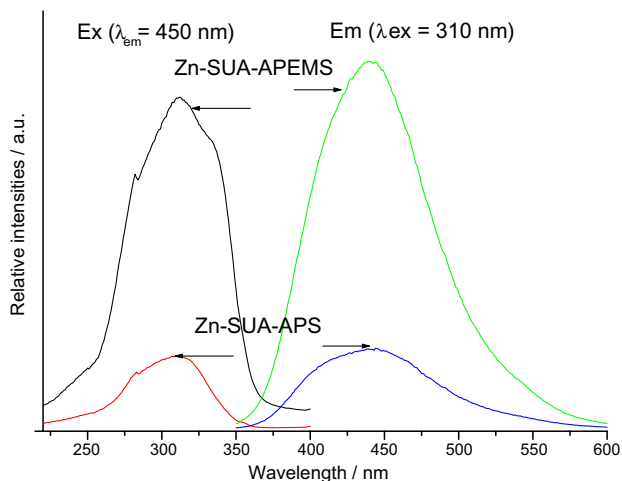


Fig. 7. The emission spectra of the zinc hybrid materials.

presents the violet luminescence with maximum wavelength of around 405 nm, while SUA-APS hybrid material shows the blue emission with maximum wavelength at 460 nm. This suggests that the different Si–O unit of APEMS and APS has influence on the luminescence position of the hybrid materials. For Fig. 7, both of the two zinc hybrids show the similar luminescent feature to the hybrids without metal ions. The luminescence principle of zinc hybrids is different from that of lanthanide molecular hybrids. Lanthanide molecular hybrids based on the intra-molecular energy transfer between ligand systems to  $\text{Ln}^{3+}$ , but the luminescence zinc molecular hybrid systems derived from the ligands are influenced by the disturbance of  $\text{Zn}^{2+}$ . Different from the emission spectra of SUA-APEMS and SUA-APS, the two zinc hybrids shows the similar blue luminescence with maximum wavelength of around 450 nm, suggesting that the disturbance of  $\text{Zn}^{2+}$  has great influence on the emission of SUA-APEMS. The zinc hybrid materials also show the stronger emission intensity, which also suggests the disturbance of  $\text{Zn}^{2+}$ .

Fig. 8 illustrates the typical photoluminescence spectra of the europium hybrid materials. The excitation spectra of Eu-SUA-APEMS and Eu-SUA-APS show the two main excitation bands, one is ascribed to the CTS and SUA modified Si–O host, the other corresponds to the f–f transition of  $\text{Eu}^{3+}$ . It is found that the two excitation bands show the similar weak intensities, suggesting

the energy transfer is not effective between the organically modified (SUA unit) Si–O host and  $\text{Eu}^{3+}$ . Generally, 5-sulfosalicylic acid is not suitable for the luminescence of  $\text{Eu}^{3+}$  for the higher energy difference [34]. All these emission spectra exhibit that the emission consisting of the  ${}^5\text{D}_0 \rightarrow {}^7\text{F}_1$ ,  ${}^5\text{D}_0 \rightarrow {}^7\text{F}_2$ , transitions at 588, 614 nm, respectively, of  $\text{Eu}^{3+}$  can be obviously obtained and the red emission ( ${}^5\text{D}_0 \rightarrow {}^7\text{F}_2$ ) possesses the strongest intensity. But a prominent phenomenon that should be noticed in these spectra is the intensity ratios  $I_{02}({}^5\text{D}_0 \rightarrow {}^7\text{F}_2)/I_{01}({}^5\text{D}_0 \rightarrow {}^7\text{F}_1)$ . In these europium hybrid materials, from SUA-APEMS-Eu to SUA-APS-Eu, the intensity ratios  $I_{02}({}^5\text{D}_0 \rightarrow {}^7\text{F}_2)/I_{01}({}^5\text{D}_0 \rightarrow {}^7\text{F}_1)$  are 1.322 and 2.133, respectively.  ${}^5\text{D}_0 \rightarrow {}^7\text{F}_1$  transition is magnetic-dipolar transitions and insensitive to their local structure environment while  ${}^5\text{D}_0 \rightarrow {}^7\text{F}_2$  transition is electric-dipolar transitions and sensitive to the coordination environment of the  $\text{Eu}^{3+}$  ion. Usually the intensity ratio of  ${}^5\text{D}_0 \rightarrow {}^7\text{F}_2$  to  ${}^5\text{D}_0 \rightarrow {}^7\text{F}_1$  is regarded as a probe to detect the inversion environmental symmetry around  $\text{Eu}^{3+}$ . If the  $\text{RE}^{3+}$  ions occupy the host sites with inversion symmetry, optical transitions inside the 4fn configuration are strictly forbidden as electric dipole transition. So it can be concluded that the  $\text{Eu}^{3+}$  ion is not located at the site with inversion symmetry. Besides, there exists apparent emission in the short wavelength region of 450–550 nm, which may be ascribed to the emission of the Si–O network. The occurrence of host'

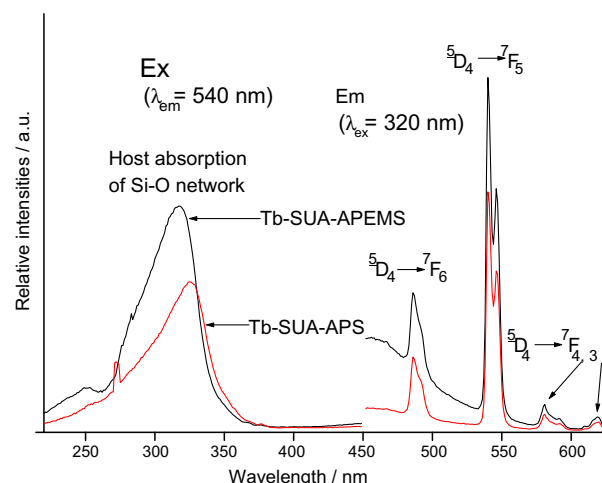


Fig. 9. The emission spectra of the terbium hybrid materials.

luminescence also verifies that the energy transfer from Si–O network host to  $\text{Eu}^{3+}$  is not effective [35,36].

The excitation and emission spectra of the resulting terbium hybrid materials are shown in Fig. 9. Different from the excitation spectra of Eu hybrids, two strong broad excitation bands can be observed, corresponding to the host absorption of Si–O network, while the f–f excitation bands are too weak to be checked. This indicates that the energy transfer from the host absorption of Si–O network and  $\text{Tb}^{3+}$  is effective. Subsequently, the strong green luminescence can be observed in their emission spectra excited by 320 nm. The emission lines of the hybrid materials were assigned to the transitions from the  ${}^5\text{D}_4 \rightarrow {}^7\text{F}_j$  ( $J=6, 5, 4, 3$ ) transitions at around 485, 540(548), 580 and 618 nm for terbium ions. Among these emission peaks, the green luminescence ( ${}^5\text{D}_4 \rightarrow {}^7\text{F}_5$ ) was most striking, which indicated that the effective energy transfer took place between the SUA-APEMS (APS) and the chelated Tb ions. It is obviously different between the intensities of the green and the blue emission since the green emission was stronger than that of the blue one. The reason may be that the emission to  ${}^5\text{D}_4 \rightarrow {}^7\text{F}_6$  is an electronic dipole transition, which is greatly influenced by the ligand field, while the emission to  ${}^5\text{D}_4 \rightarrow {}^7\text{F}_5$  belongs to a magnetic dipole transition, which is less influenced by the ligand field. Besides, these bands in the short wavelength region cannot be clearly found in the spectra of terbium hybrids, suggesting that there exist more effective energy transfer process in the terbium hybrids than europium ones.

The typical decay curve of these two  $\text{Eu}^{3+}$  hybrid materials were measured and they can be described as a single exponential ( $\ln(S(t)/S_0) = -k_1t = -t/\tau$ ), indicating that all  $\text{Eu}^{3+}$  ions occupy the same average coordination environment. The resulting lifetime data of  $\text{Eu}^{3+}$  hybrid materials were given in Table 1. Furtherly, we selectively determined the emission quantum efficiencies of the  ${}^5\text{D}_0$  excited state of europium ion for  $\text{Eu}^{3+}$  hybrids on the basis of the emission spectra and lifetimes of the  ${}^5\text{D}_0$  emitting level, the detailed luminescent data were shown in Table 1. The quantum efficiency of the luminescence step,  $\eta$  expresses how well the radiative processes (characterized by rate constant  $A_r$ ) compete with non-radiative processes (overall rate constant  $A_{nr}$ ) [37–41].

$$\eta = A_r / (A_r + A_{nr}) \quad (1)$$

Non-radiative processes influence the experimental luminescence lifetime by the equation:

$$\tau_{\text{exp}} = (A_r + A_{nr})^{-1} \quad (2)$$

**Table 1**  
The luminescence efficiencies and lifetimes of the europium covalent hybrids.

Systems	Eu–M <sub>1</sub>	Eu–M <sub>2</sub>
$\tau$ (ms)	0.24	0.31
$\nu_{01}$ ( $\text{cm}^{-1}$ ) <sup>a</sup>	16 965	16 996
$\nu_{02}$ ( $\text{cm}^{-1}$ ) <sup>a</sup>	16 284	16 284
$\nu_{03}$ ( $\text{cm}^{-1}$ ) <sup>a</sup>	15 383	15 314
$\nu_{04}$ ( $\text{cm}^{-1}$ ) <sup>a</sup>	14 278	14 342
$I_{01}$ <sup>b</sup>	129.6	306.7
$I_{02}$ <sup>b</sup>	257.4	410.548
$I_{03}$ <sup>b</sup>	13.215	48.9
$I_{04}$ <sup>b</sup>	13.1	40.216
$A_{01}$ ( $\text{s}^{-1}$ )	50	50
$A_{02}$ ( $\text{s}^{-1}$ )	103.5	69.8
$A_{03}$ ( $\text{s}^{-1}$ )	5.6	8.8
$A_{04}$ ( $\text{s}^{-1}$ )	6.02	7.8
$A_{\text{rad}}$ ( $\text{s}^{-1}$ )	213.9	136.4
$\eta$ (%)	4.0	4.3

<sup>a</sup> The energies of the  ${}^5\text{D}_0 \rightarrow {}^7\text{F}_j$  transitions ( $\nu_{0j}$ ).

<sup>b</sup> The integrated intensity of the  ${}^5\text{D}_0 \rightarrow {}^7\text{F}_j$  emission curves.

So quantum efficiency can be calculated from radiative transition rate constant and experimental luminescence lifetime from the following equation:

$$\eta = A_r \tau_{\text{exp}} \quad (3)$$

where  $A_r$  can be obtained by summing over the radiative rates  $A_{0j}$  for each  ${}^5\text{D}_0 \rightarrow {}^7\text{F}_j$  transitions of  $\text{Eu}^{3+}$ .

$$A_r = \sum A_{0j} = A_{00} + A_{01} + A_{02} + A_{03} + A_{04} \quad (4)$$

The branching ratio for the  ${}^5\text{D}_0 \rightarrow {}^7\text{F}_{5,6}$  transitions can be neglected as they both are not detected experimentally, whose influence can be ignored in the depopulation of the  ${}^5\text{D}_0$  excited state. Since  ${}^5\text{D}_0 \rightarrow {}^7\text{F}_1$  belongs to the isolated magnetic dipole transition, it is practically independent of the chemical environments around the  $\text{Eu}^{3+}$  ion, and thus can be considered as an internal reference for the whole spectrum, the experimental coefficients of spontaneous emission,  $A_{0j}$  can be calculated according to the equation.

$$A_{0j} = A_{01} (I_{0j}/I_{01}) (\nu_{01}/\nu_{0j}) \quad (5)$$

Here  $A_{0j}$  is the experimental coefficients of spontaneous emissions, among  $A_{01}$  is the Einstein's coefficient of spontaneous emission between the  ${}^5\text{D}_0$  and  ${}^7\text{F}_1$  energy levels. In vacuum,  $A_{01}$  as a value of  $14.65 \text{ s}^{-1}$ , when an average index of refraction  $n$  equal to 1.506 was considered, the value of  $A_{01}$  can be determined to be  $50 \text{ s}^{-1}$  approximately ( $A_{01} = n^3 A_{01(\text{vacuum})}$ ).  $I$  is the emission intensity and can be taken as the integrated intensity of the  ${}^5\text{D}_0 \rightarrow {}^7\text{F}_j$  emission bands.  $\nu_{0j}$  refers to the energy barycenter and can be determined from the emission bands of  $\text{Eu}^{3+}$ 's  ${}^5\text{D}_0 \rightarrow {}^7\text{F}_j$  emission transitions. Here the emission intensity,  $I$ , taken as integrated intensity  $S$  of the  ${}^5\text{D}_0 \rightarrow {}^7\text{F}_{0-4}$  emission curves, can be defined as below:

$$I_{i-j} = h\omega_{i-j} A_{i-j} N_i \approx S_{i-j} \quad (6)$$

where  $i$  and  $j$  are the initial ( ${}^5\text{D}_0$ ) and final levels ( ${}^7\text{F}_{0-4}$ ), respectively,  $\omega_{i-j}$  is the transition energy,  $A_{i-j}$  is the Einstein's coefficient of spontaneous emission, and  $N_i$  is the population of the  ${}^5\text{D}_0$  emitting level. On the basis of the above discussion, the quantum efficiencies of these two kinds of europium hybrid materials can be calculated and the related data and the result were also given in Table 1. From the equation of  $\eta$ , it can be seen the value  $\eta$  mainly depends on the values of two quantum parameters: lifetimes and red/orange ratio ( $I_{02}/I_{01}$ ). If the lifetimes and red/orange ratio are large, the quantum efficiency must be high. So the different composition of the hybrid materials may have influence on the luminescent lifetimes and quantum efficiencies.

The scanning electron micrographs of Eu-SUA-APEMS, Tb-SUA-APEMS are shown in Fig. 10. These images for the hybrid materials demonstrate that homogeneous, molecular-based materials were obtained where no phase separation was observed because of strong covalent bonds bridging between the inorganic and organic phases which belong to a complicated huge molecule in nature, and that they are composed quite uniformly so that the two phases can exhibit their distinct properties together. On the surface of these hybrid materials, uniform cuboid particles can be observed. These phenomena are mostly attributed to the sol–gel treatment. In the sol process, the o/w macro-emulsion is decisive and responsibility for the materials' final texture. The isolated cube is easy to understand because the weak interactions between the organic moieties such as van der Waals, London, or  $\pi$ – $\pi$  stacking were able to induce an organization [42–44]. Ultimately, compared with the two SEM pictures, the uniform cuboid particles on the surface of Tb-SUA-APEMS system are closer to the rectangular cube, which may be due to the difference of the precursor molecules.

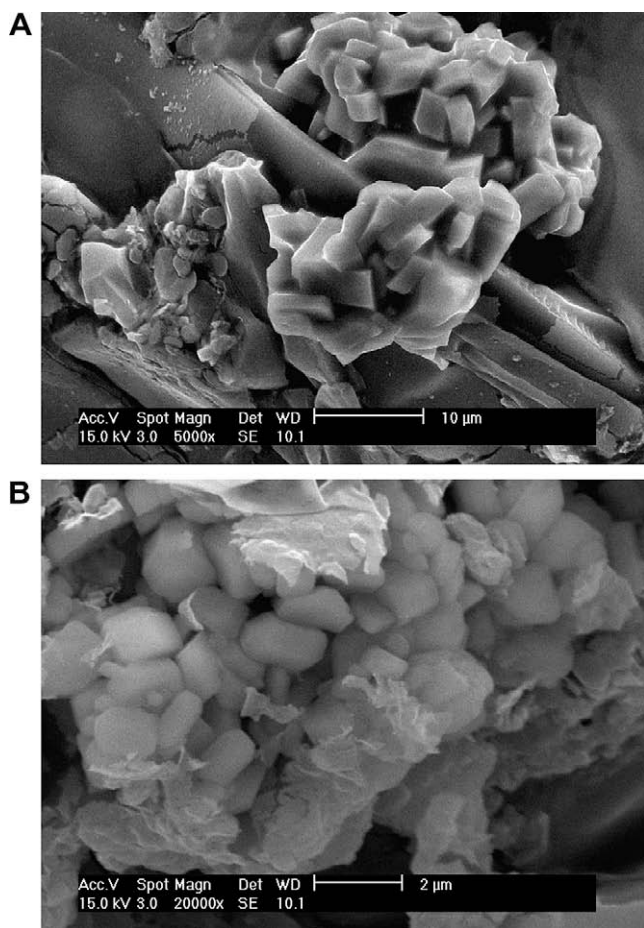


Fig. 10. The scanning electron micrographs of Eu-SUA-APEM (A), Tb-SUA-APEM (B).

#### 4. Conclusion

In summary, a new series of luminescent molecular-based hybrid materials was firstly achieved via a special sol–gel process. It is based on the modification of 5-sulfosalicylic acid with APMS and APS, which shows the characteristic luminescence and uniform microstructure. The modification of sulfonic acid seems to be neglected in the hybrid materials area. But numerous compounds containing sulfonic group are expected to be introduced into the hybrids in this way because the hybrid materials derived from the 5-sulfosalicylic modification have excellent optical, physical and chemical properties.

#### Acknowledgements

This work was supported by the National Natural Science Foundation of China (20671072) and Program for New Century Excellent Talents in University (NCET-08-0398).

#### References

- [1] G. Blass, B.C. Grabmaier (Eds.), *Luminescent Materials*, Springer, Berlin, 1994.
- [2] S. Hufner, *Optical Spectra of Transparent Rare Earth Compounds*, Academic Press, New York, 1978.
- [3] M.P. Bailey, B.F. Rocks, C. Riley, *Analyst* 109 (1984) 1449.
- [4] J.C.G. Bunzli, F. Ihringer, *Inorg. Chim. Acta* 246 (1996) 195.
- [5] P.K. Sharma, A.R. van Doom, A.G.J. Staring, *J. Lumin.* 62 (1994) 219.
- [6] F.R.G.E. Silva, J.F.S. Menezes, G.B. Rocha, S. Alves, H.F. Brito, R.L. Longo, O.L. Malta, *Coord. Chem. Rev.* 303 (2000) 364.
- [7] H. Takkalo, V.M. Mukkala, L. Merio, J.C. Rodriguez-Ubis, R. Sedano, O. Juanes, E. Brunet, *Helv. Chim. Acta* 80 (1997) 372.
- [8] G.F. de Sa, L.H.A. Nunes, Z.M. Wang, G.R. Choppin, *J. Alloys Compd.* 196 (1993) 17.
- [9] N. Sabbatini, M. Guardigli, J.M. Lehn, *Coord. Chem. Rev.* 123 (1993) 201.
- [10] J.C.G. Bunzli, P. Froidevaux, J.M. Harrowfield, *Inorg. Chem.* 32 (1993) 3306.
- [11] B. Yan, H.J. Zhang, C.G. Xu, T.L. Chen, J.Z. Ni, *Spectrosc. Lett.* 33 (2000) 705.
- [12] M. Pietraszkiewicz, J. Karpiuk, A.K. Rout, *Pure Appl. Chem.* 65 (1993) 563.
- [13] S. Petoud, J.C.G. Bunzli, K.J. Schenk, C. Piguet, *Inorg. Chem.* 36 (1997) 1345.
- [14] W.W. Horrocks De Jr., P. Bolender, W.D. Smith, R.M. Supkowski, *J. Am. Chem. Soc.* 119 (1997) 5972.
- [15] J.H. Harreld, A. Esaki, G.D. Stucky, *Chem. Mater.* 15 (2003) 3481.
- [16] P.N. Minoofar, R. Hernandez, S. Chia, B. Dunn, J.I. Zink, A.C. Franville, *J. Am. Chem. Soc.* 124 (2002) 14388.
- [17] J. Choi, R. Tamaki, S.G. Kim, R.M. Laine, *Chem. Mater.* 15 (2003) 3365.
- [18] A.C. Franville, D. Zambon, R. Mahiou, S. Chou, Y. Troin, J.C. Cousseins, *J. Alloys Compd.* 275–277 (1998) 831.
- [19] A.C. Franville, R. Mahiou, D. Zambon, J.C. Cousseins, *Solid State Sci.* 3 (2001) 211.
- [20] A.C. Franville, D. Zambon, R. Mahiou, Y. Troin, *Chem. Mater.* 12 (2000) 428.
- [21] H.R. Li, J. Lin, H.J. Zhang, L.S. Fu, Q.G. Meng, S.B. Wang, *Chem. Mater.* 14 (2002) 3651.
- [22] H.R. Li, J. Lin, H.J. Zhang, H.C. Li, L.S. Fu, Q.G. Meng, *Chem. Commun.* (2001) 1212.
- [23] Q.M. Wang, B. Yan, *J. Mater. Chem.* 14 (2004) 2450.
- [24] Q.M. Wang, B. Yan, *J. Photochem. Photobiol. A: Chem.* 178 (2006) 70.
- [25] Q.M. Wang, B. Yan, *Cryst. Growth Des.* 5 (2005) 497.
- [26] Q.M. Wang, B. Yan, *J. Mater. Res.* 20 (2005) 592.
- [27] B. Yan, D.J. Ma, *J. Solid State Chem.* 179 (2006) 2059.
- [28] B. Yan, X.F. Qiao, *Photochem. Photobiol.* 83 (2007) 971.
- [29] C. Sanchez, F. Ribot, *New J. Chem.* 18 (10) (1994) 1007.
- [30] R. Corriu, D. Leclercq, *Angew. Chem., Int. Ed. Engl.* 35 (1996) 1420.
- [31] E. Pretsch, P. Buhlmann, C. Affolter (Eds.), *Structure Determination of Organic Compounds*, 2nd ed., Springer, Berlin, 2003.
- [32] Z. Wang, J. Wang, H.J. Zhang, *Mater. Chem. Phys.* 87 (2004) 44.
- [33] Q.M. Wang, B. Yan, 2005 175 (2005) 159.
- [34] B. Yan, H.J. Zhang, S.B. Wang, J.Z. Ni, *Chem. Pap.* 52 (1998) 199.
- [35] Y. Hasegawa, M. Yamamuro, Y. Wada, N. Kanehisa, Y. Kai, S. Yanagida, *J. Phys. Chem. A* 107 (2003) 1697.
- [36] C.G. Gulgas, T.M. Reineke, *Inorg. Chem.* 44 (2005) 9829.
- [37] E.E.S. Teotonio, J.G.P. Espinola, H.F. Brito, O.L. Malta, S.F. Oliveria, D.L.A. de Faria, C.M.S. Izumi, *Polyhedron* 21 (2002) 1837.
- [38] M.H.V. Werts, R.T.F. Jukes, J.W. Verhoeven, *Phys. Chem. Chem. Phys.* 4 (2002) 1542.
- [39] O.L. Malta, M.A.C. dosSantos, L.C. Thompson, N.K. Ito, *J. Lumin.* 69 (1996) 77.
- [40] G.F. de Sa, O.L. Malta, C.D. Donega, A.M. Simas, R.L. Longo, P.A. Santa-Cruz, E.F. da Silva, *Coord. Chem. Rev.* 196 (2000) 165.
- [41] J.C. Boyer, F. Vetrone, J.A. Capobianco, A. Speghini, M. Bettinelli, *J. Phys. Chem. B* 108 (2004) 20137.
- [42] B. Boury, F. Ben, R.J.P. Corriu, P. Delord, M. Nobili, *Chem. Mater.* 14 (2002) 730.
- [43] M.C. Goncalves, V.D. Bermudez, R.A. Sa Ferreira, L.D. Carlos, D. Ostrovskii, J. Rocha, *Chem. Mater.* 16 (2004) 2530.
- [44] B. Boury, R.J.P. Corriu, *Chem. Commun.* (2002) 795.